Proceedings World Geothermal Congress 2020+1
Reykjavik, Iceland, April - October 2021

Hydraulic Stimulation Design for Well RV-43 on Geldinganes, Iceland

Hannes Hofmann, Günter Zimmermann, Arno Zang, Santiago Aldaz, Simone Cesca, Sebastian Heimann, Stefan Mikulla, Claus Milkereit, Torsten Dahm, Ernst Huenges

Helmholtz Centre Potsdam GFZ German Research Centre for Geosciences, Potsdam, Germany

Vala Hjörleifsdóttir, Sandra Osk Snæbjörnsdóttir, Edda Sif Aradóttir

Reykjavik Energy, Reykjavik, Iceland

Ragnheidur St. Ásgeirsdóttir, Kristján Ágústsson, Rögnvaldur Magnússon, Stefán Auðunn Stefánsson, Ólafur Flovenz

ISOR, Reykjavik, Iceland

Arnaud Mignan, Marco Broccardo, Antonio Pio Rinaldi, Luca Scarabello, Dimitrios Karvounis, Francesco Grigoli, Stefan Wiemer

Swiss Seismological Service, ETH-Zurich, Zurich, Switzerland

Sveinbjörn Hólmgeirsson

GeoEnergy Consulting, Reykjavik, Iceland

hannes.hofmann@gfz-potsdam.de

Keywords: Enhanced Geothermal Systems, soft stimulation, cyclic injection, multi-stage stimulation, Iceland, risk assessment, seismic monitoring, traffic light system

ABSTRACT

The district heating system of the city of Reykjavik is almost exclusively fed by geothermal energy. Due to a growing population and increasing heat demand new heat sources need to be connected to the existing district heating network. One of the remaining potential geothermal systems with suitable conditions can be found on Geldinganes, an uninhabited peninsula within the city limits of Reykjavik. The only production well, RV-43, found the required temperatures, but not the necessary flow rates for economic heat production. Therefore, it is planned to develop this geothermal field by drilling new wells into potentially more permeable zones. Additionally, it is anticipated to hydraulically stimulate the existing well RV-43 in order to improve its hydraulic performance and to add additional production from this well to the heat network. Due to the location of the well within the city limits of Reykjavik, hydraulic stimulation treatments have to be designed to maximize the hydraulic performance increase while minimizing potential environmental risks such as induced seismicity. We provide an overview of the project including the site assessment, conceptual model, planned pre- and post-stimulation measurements, treatment schedule, zonal isolation and multi-stage injection concept, seismic monitoring network and procedures, and seismic risk assessment and seismic risk mitigation procedures, such as the cyclic soft stimulation concept and a site specific traffic light system.

1. INTRODUCTION

Reykjavik, the capital and center of population of Iceland, meets 99.9% of its district heating demand by geothermal energy (Gunnlaugsson et al. 2000). This energy is provided through two separate networks. One network is fed by two high temperature power plants, the Nesjavellir power plant and the Hellisheiði Power Plant, both 20-30 km east of Reykjavik. The second and the oldest network is fed by three low temperature fields (Laugarnes, Ellidaar, Mosfellssveit) within or near the city limits. However, the growing population and number of tourists in the city of Reykjavik in Iceland pushes the current network at its limit. This is because no new low temperature wells have been drilled since 2001 despite the increase in demand. In particular, additional sources of low temperature heat need to be accessed to ensure a reliable heat provision for the city centre. Therefore, the current capacity has to be increased by drilling new low temperature wells and stimulating older inactive wells.

One potential area for new low temperature geothermal field developments is Geldinganes. Geldinganes is a peninsula within the city limits of Reykjavik. The exceptional geothermal gradient in this area triggered the drilling of well RV-43 in 2001 after a gabbro body was identified as potential heat source and drilling target for this deviated well (Figure 1). While the required temperatures were found, the flow rates were insufficient for economic production. The initial production rates of 2-3 l/s could be increased to ~10 l/s by an open hole stimulation treatment that was performed directly after drilling in 2001. This was considered as uneconomic at that time as it was the only producer in the area and the network connection was some kilometers away. Currently, this field is re-assessed for development with new production wells. To additionally enhance the production from this field it is foreseen to hydraulically stimulate well RV-43 again in order to improve its productivity to economic levels.

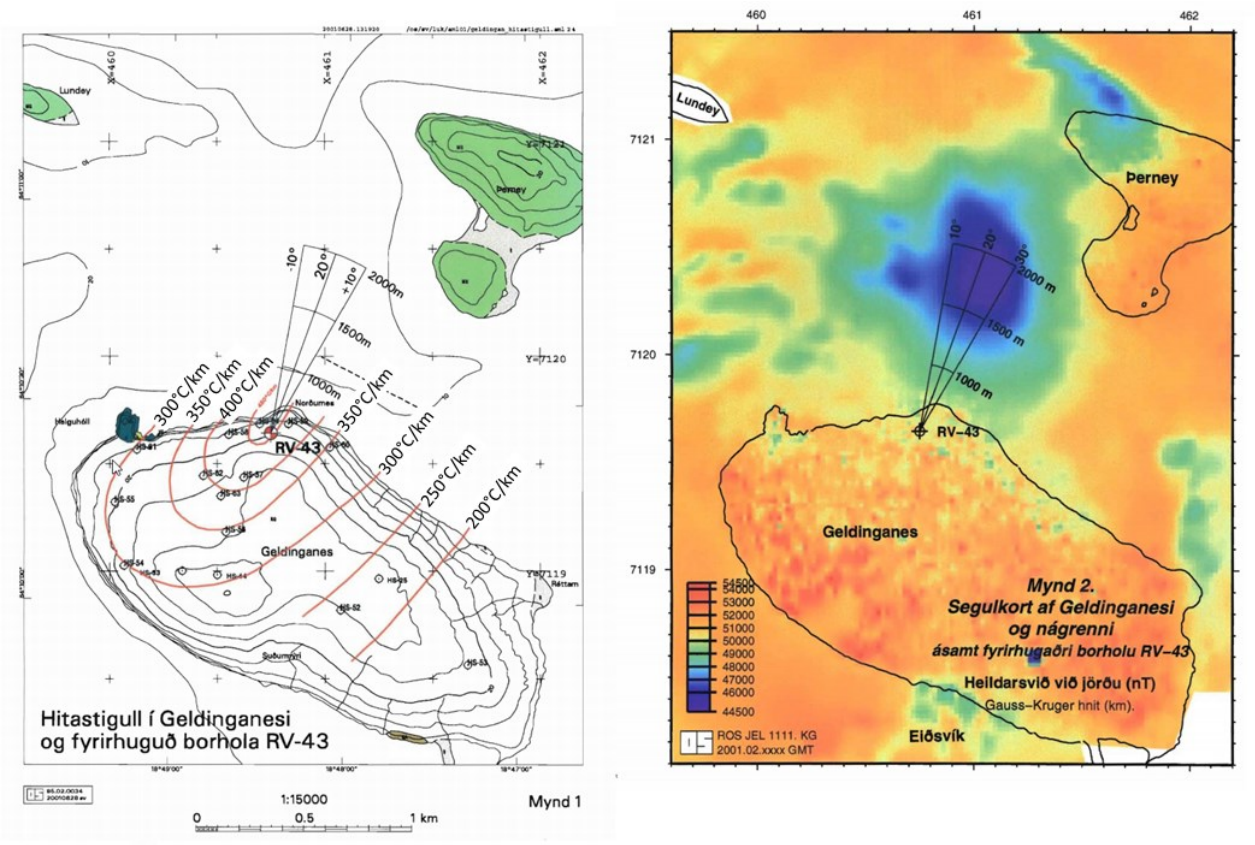

Figure 1: Temperature gradient map (left, Steingrímsson et al. 2001) and magnetic map (right, Gunnarsson 2001) of Geldinganes and location of well RV-43.

Hydraulic stimulation has been a routine procedure to improve the productivity of low temperature geothermal wells in the Reykjavik area since the 1970s. Stimulations were performed with single injection packers, flow rates of 15 to 100 l/s and pressures of a few to 15 MPa at 15 l/s. Compared to the estimated productivity of the wells after drilling this resulted in a thirty to fourty fold improvement of productivity. Compared to productivity estimates from the total loss of circulation during drilling the improvement was up to three fold. This productivity increase was attributed to re-opening of production zones that were plugged during drilling, removal of zeolite and calcite vein deposits and permeability increase of hyaloclastic rocks in the near wellbore areas. In the Mosfellssveit area alone at least 38 wells have been hydraulically stimulated in the past (Tomasson and Thorsteinsson 1978). Additional hydraulic stimulations in Reykjavik are reported for the Seltjarnes low temperature field (Tulinius et al. 1996). Two hydraulic fracturing treatments were performed at shallow depths in Reykjavik as well (Haimson and Voight 1977).

Even though no induced seismic activity was reported or found in relation to any of these fluid injection activities in the past, special emphasize is given on seismic risk assessment and mitigation in the upcoming stimulation project for well RV-43. This is because the well is in close proximity to the most populated area of Iceland, the seismic activity in Iceland is generally high and induced seismicity recently became a challenge and matter of public concern at other geothermal areas in seismically more active areas of Iceland (e.g., Hellisheidi; Bessason et al. 2012).

For this reason, the project is accompanied scientifically by the EU H2020 project DESTRESS (Huenges et al., 2020). Within the framework of this project, so called “soft stimulation treatments” of geothermal reservoirs are demonstrated in several geological environments. Soft stimulation treatments aim to achieve enhanced reservoir performance while minimizing environmental impacts such as induced seismicity. At well RV-43 the cyclic soft stimulation treatment will be demonstrated (Hofmann et al. 2018). The stimulation design includes cyclic injection, progressive flow rate changes, monitoring injection volumes, flow back instead of shut-in, multi-stage injection, and a seismic traffic light system. The stimulation will be accompanied by a real-time seismic monitoring system and in addition to a conventional traffic light system, an advanced traffic light system, developed within the framework of DESTRESS, will be applied for the first time in the field. The site operations will also be accompanied by geochemical monitoring and numerical modeling, which are not described here. In this paper, site assessment, risk assessment results, risk mitigation procedures, stimulation design and monitoring concept will be summarized.

2. SITE ASSESSMENT

2.1 Well RV-43

The deviated well RV-43 was drilled in 2001 with an average inclination and azimuth of the 1130 m long open hole section of ~38° and ~N20°E, respectively. The measured depth (MD) of the well is 1832 m and the corresponding true vertical depth (TVD) is ~1,550 m. The kick off point is at ~270 m and the horizontal distance between wellhead and bottom hole of well RV-43 is ~810 m. Three casings were installed: a 18 5/8” surface casing down to 48 m MD, a 13 3/8” anchor casing down to 252 m MD, and a 9 5/8“

production casing down to 702 m MD. There is no liner in the well; it is open from 702 to 1832 m MD with an open hole diameter of 8 ½". The wellbore is currently not accessible by wireline logging tools below ~830 m MD.

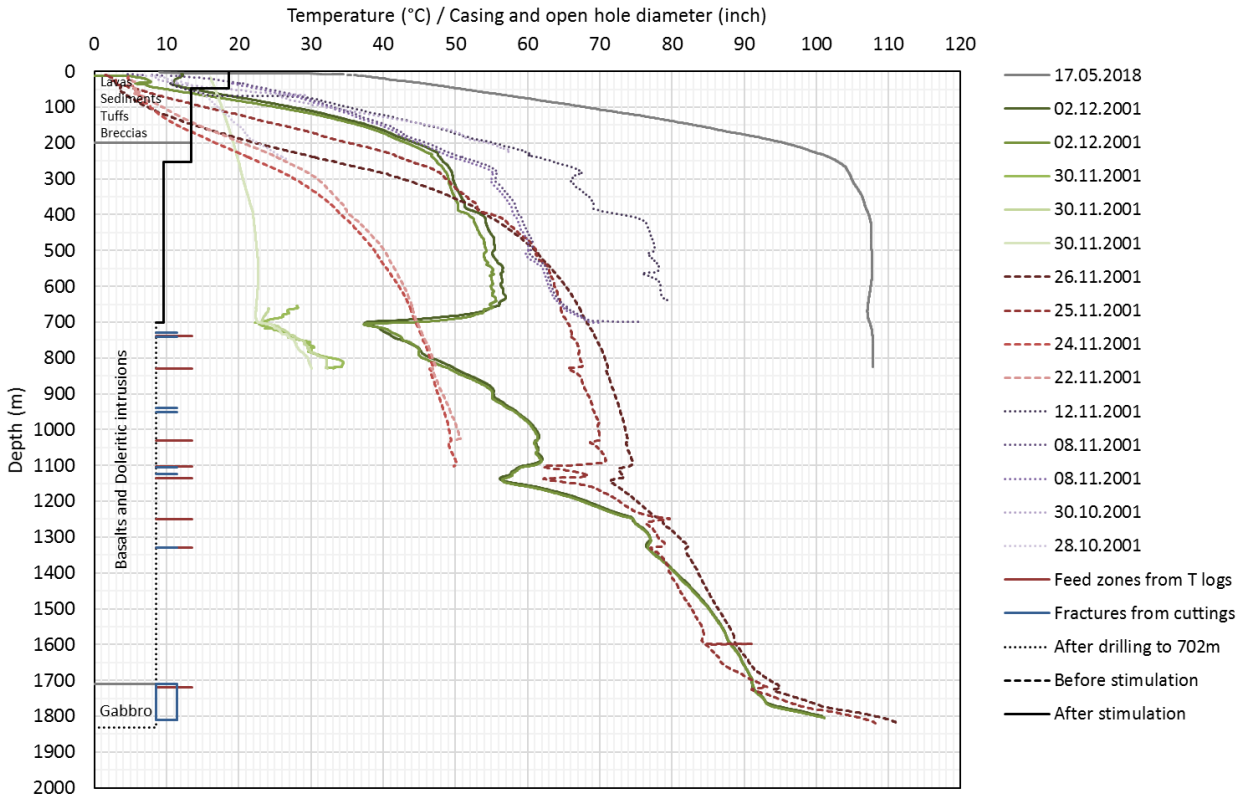

Figure 2: Temperature logs, completion, feed zones and fractures of well RV-43.

The largest part of well RV-43 intersected medium-coarse grained basalts, mostly intrusives. Above 200 m lavas and sediments are found, along with some tuffs and breccias that erupted during glaciations. Below 200 m there are almost solely intrusives and lavas, but some layers of brecciated rocks. Doleritic intrusions comprise the majority of the strata. The intrusive rocks are usually less altered than their host rocks (lava piles), which are usually highly altered. The intrusions however differ in alteration indicating different relative ages of these rocks. These could be cone sheets which are one of the characteristics of central volcanos. The lithology changes somewhat in the bottom part of the well between ~1710-1810 m MD. The cuttings at this depth are comprised of a high fraction of lightly colored minerals, including some amount of coarse grained primary minerals and metals. XRD analysis revealed that the majority of the cuttings were anorthite, with some quartz and albite. This indicates that a gabbroic intrusion was intersected at this depth, probably the gabbro revealed NW of Geldinganes in the gravimetric and magnetic measurements carried out outside of the Geldinganes peninsula. This more coarse-grained gabbro body was the target of well RV-43.

The rocks intersected in the well are mostly moderately or highly altered. The most abundant alteration minerals are pyrite, calcite and laumontite. The formation temperatures (the temperatures required for the formation of specific minerals) of the secondary minerals detected in the well can reveal the alteration history of the area. Stilbite is detected in the top 120 m (temperature below 60°C), but below 120 m it is replaced with laumontite (formation temperature of 100-120°C) which is detected in samples down to the bottom of the well. Higher degrees of alteration are also detected, indicating that laumontite is the most recently formed alteration mineral in a cooling system which previously experienced much higher temperatures. Quartz is common in the well, indicating temperatures above 180°C. Epidote is detected sporadically from ~700-1300 m MD, and is quite common below 1300 m MD, but epidote indicates formation temperatures above 240°C. The epidote is almost always overprinted by laumontite. This indicates that the present temperature within the well is ~100-150°C, which agrees with recent temperature measurements (Figure 2).

Almost no loss of circulation was observed during drilling of the well. Some losses occurred below ~1700 m, but no large feed zones were identified. Minor feed zones were located at ~738 m, ~830 m, ~1030 m, ~ 1102 m, ~ 1135 m, ~1250 m, ~ 1330 m and ~1720 m MD based on temperature logs run after drilling. From cuttings analysis, it was obvious that some mostly impermeable fractures filled with secondary minerals were intersected. These fractures were located at ~730-740 m, ~940-950 m, ~1105 m, ~1125 m, ~1330 m, and ~1710-1810 m MD (Figure 2).

After drilling of the well, an air lift was performed. The well started flowing at 1.9 MPa wellhead pressure (WHP), with flow rates of ~2-3 l/s. Temperature logs run after drilling identified the inflow zone to be at ~1100 m MD. To increase the productivity of the well a hydraulic stimulation treatment was performed over ~3 days with flow rates between 40 and 60 l/s and WHPs of 6.6 to 10 MPa. An airlift test after the stimulation showed an increase of production rates from ~2-3 l/s to ~10 l/s at similar pressure draw down. Temperature logging performed after the pumping revealed that most of the water had flowed through feed zones just below

the end of the casing at >702 m MD, and only a small fraction of the injected water had reached a feed zone at about 1250 m MD. No water had reached the deeper parts of the well.

2.2 Structural geology

The faults mapped at the surface within a 10 km radius around the site may be divided into two (sub)-vertical sets of normal faults (Gudmundsson et al. 1992) dipping towards NW-W (Figure 3). Based on digitized faults from the geological map from ISOR (Saemundsson et al. 2016) set 1 strikes ~42° (+-8°) and set 2 strikes ~5° (+-3°). Similar trends were reported by Jefferis and Voight (1981). On the peninsula Geldinganes no clear faults were mapped, but shallow temperature measurements show an increased temperature gradient along a similar strike as fault set 1 (Figure 1 and Figure 3), which is also similar to the strike of regional faults located >10 km from the site (Saemundsson et al. 2016).

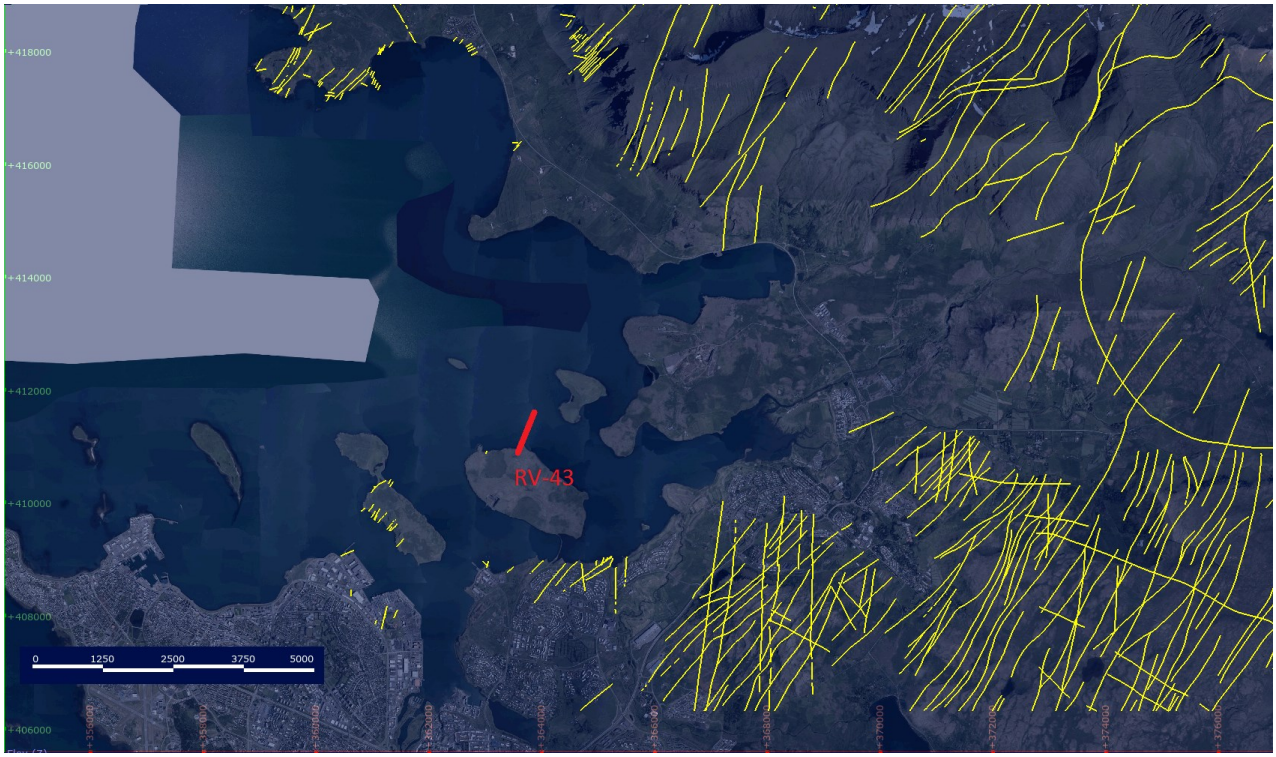

Figure 3: Fault traces from Saemundsson et al. (2016) and path of well RV-43. The (sub-)vertical normal faults may be divided into two sets striking ~42° and ~5°.

2.3 Stress field

The stress regime at depth in Geldinganes is expected to be primarily a normal faulting regime. This is indicated by hydraulic fracturing stress measurements in nearby well H32 (Haimson and Voight 1977). At shallow depth and locally strike-slip or even reverse faulting components may exist as indicated by shallow hydraulic fracturing stress measurements in nearby well H18 (Haimson and Voight 1977). Based on stress inversions of focal mechanism solutions, geological indicators and one of the hydraulic fracturing stress measurements the maximum horizontal stress direction in SW Iceland is primarily NE-SW (Gudmundsson et al. 1992; Heidbach et al. 2016; Ziegler et al. 2016). This is also supported by GPS measurements and resulting extensional and contractional horizontal strain rates (Keiding et al. 2009). Locally, this direction may vary between NW-SE and NE-SW as indicated by the hydraulic fracturing measurements in H18 and H32 in Reykjavik (Haimson and Voight 1977). Based on the twelve stress indicators within a radius of ~10 km around the site with poor data quality (C-D), the maximum horizontal stress direction may range between N45°W and N37°E (Heidbach et al. 2016). The maximum horizontal stress direction in the paleostress field was determined to be between N20°E and N40°E based on fault slip data from SW Iceland (Gudmundsson et al. 1992). The elevated temperature gradient on Geldinganes that strikes NE-SW (Figure 1) supports the hypothesis that the local stress field on Geldinganes is similar to the regional stress field with the maximum horizontal stress direction being NE-SW (~N30°E). Borehole televiewer (BHTV) measurements will allow to further constrain the local stress field before the planned stimulation treatment.

Haimson and Voight (1976) determined the stress gradients from four hydraulic fracturing tests in well H32 between 200 and 375 m depth (z) and from three hydraulic fracturing tests in well H18 between 180 and 324 m depth. The results were: ΔSV [MPa] = 27 MPa/km x z [km], $\Delta SHmax$ [MPa] = 3 MPa + 30 MPa/km x z [km], $\Delta Shmin$ [MPa] = 21 MPa/km x z [km]. Linear trends through the original data from both wells (published by Haimson and Voight 1977) may be an alternative interpretation of the stress field on Geldinganes (Figure 4). The two measurements in Dolerite with increased mimimum horizontal stress gradients are neglected for this. The resulting stress gradients are: ΔSV [MPa] ~ 27 MPa/km x z [km], $\Delta SHmax$ [MPa] ~ (3 MPa + 13 MPa/km x z [km]), $\Delta Shmin$ ~ (2 MPa + 10.5 MPa/km x z [km]). The pore pressure gradient of ~9.8 MPa/km is assumed to be hydrostatic with a fluid density of 1,000 kg/m³. The corresponding stresses at target depths are summarized in Table 1.

Intrusive Dolerites showed an increased SHmax magnitude as compared to hydraulic fracturing stress measurements in basalts in well H18 (Haimson and Voight 1977). Haimson and Rummel (1982) found elevated stresses in thick lava flows by stress

measurements in eastern Iceland. Assuming the same behavior in RV-43 these zones may serve as fracture height growth barriers. Hemmingsen et al. (2016) conclude that horizontal stresses in Iceland are very low due to tectonic plate movements.

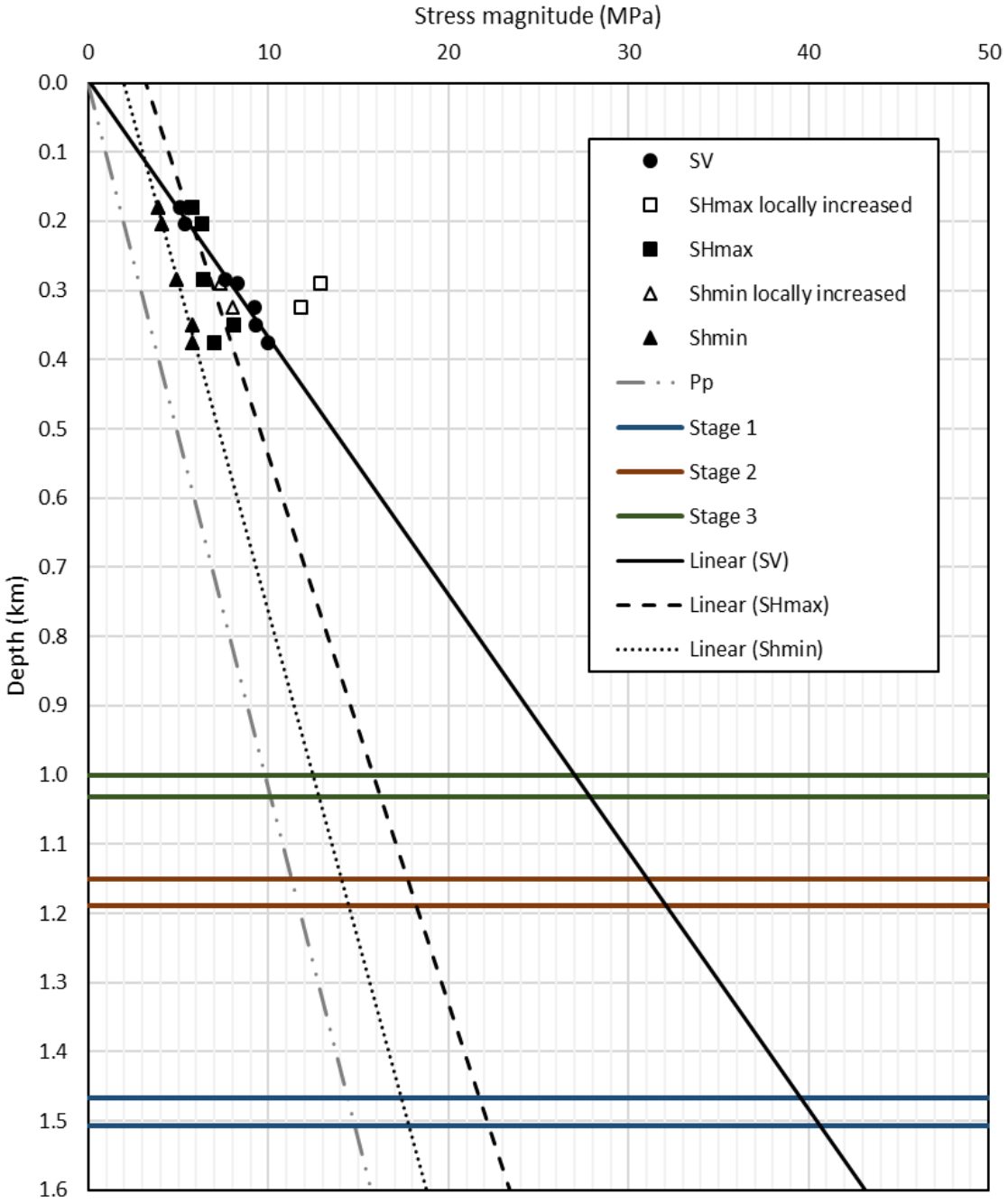

Figure 4: Stress gradients derived from shallow borehole measurements from wells H18 and H32. Note that the horizontal stresses locally increased in the two tests in dolerite. These values were omitted in the extrapolation. This is because these high stress layers are supposed to act as fracture height growth barriers surrounding the target zones of lower or average stress. The data is taken from Table 4 in Haimson and Voight (1977).

2.4 Conceptual model

Well RV-43 has a deviated open hole section with an azimuth of ~N20°E through basalts and doleritic intrusions into a gabbro body. The area is intersected by at least two (sub-)vertical sets of normal faults striking ~N42°E and ~N5°E. The maximum horizontal stress direction in this normal stress regime is assumed to be ~30°. Thus, the well azimuth is in between the two possible fault sets and similar to the maximum horizontal stress direction. It is expected that doleritic intrustions will act as stress barriers that confine fracture height growth. These sections of the well would thus be suitable for setting the packers. The stimulation targets are the fractured and altered basalts in between doleritic intrusions and the intersection of the gabbro body. Removing near wellbore damage, sustainable aperture increase of sealed fractures intersecting the wellbore and hydraulic connection of surrounding fracture networks to the wellbore are expected to be the main drivers of productivity increase. In this conceptual model hydraulic fractures would develop parallel to SHmax and thus parallel to the wellbore. This could lead to sealing problems of the packers and stability

problems of the well. However, the target is to stimulate the two pre-existing fracture sets, which are vertical and at an angle to the wellbore azimuth, below the fracturing pressure, i.e. by hydro-shearing.

3. STIMULATION DESIGN

3.1 Stimulation targets

The goal of the stimulation is a further productivity increase in addition to the productivity achieved after the hydraulic stimulation performed after drilling in 2001, where the productivity index (PI) increased from ~1.0-1.6 l/s/MPa to ~5.3 l/s/MPa. A further fold of increase (FOI) by ~2-3 with a minimum PI of ~10 l/s/MPa is the target of the stimulation. This goal is to be achieved by sealing and stimulating existing fracture zones separately through straddle packer assemblies. The anticipated stimulation mechanism is hydro-shearing. The productivity increase is expected to be a result of removing drilling induced wellbore damage and permeability increase of existing fractures by stimulation. Stimulation treatment and risk mitigation measures are designed for maximum local magnitudes of induced seismic events of 3.0 and the traffic light system applied starts to operate when seismic magnitudes reach M_L1.5. Additionally, the cyclic soft stimulation concept in combination with multi-stage stimulation will be demonstrated in the field.

3.2 Field operations schedule

1) Borehole cleaning and remedial: At first, the open hole section will be calibrated to bottom with a triconic bit and circulated through the bottom hole assembly (BHA) in order to remove debris and clean the well. Thereafter, a cased hole cleaning BHA composed of bull nose, scrapers, brush, magnets and baskets will be run downhole to clean the casing and remove remaining debris and potential cased hole obstructions to make the well accessible for wireline tools and straddle assemblies from top to bottom.

2) Airlift test: The wellbore will be further cleaned and the initial productivity will be calculated based on an airlift test.

3) Open hole logging: In order to identify intact and circular open hole sections that are suitable for setting the packers a borehole televiewer log (BHTV) will be run next. This will also allow to identify fracture zones as potential stimulation targets and information on borehole breakouts or drilling induced fractures will provide additional constraints to the stress field estimation. This log will be combined with gamma ray, spontaneous potential, resistivity and temperature log to identify current inflow zones.

4) Stimulation: Three main stages will be stimulated separately with a hydraulic straddle assembly. The assembly is positioned in the open hole section and activated with a ball-drop inflation mechanism. Once the inflatable packers are positioned, set and tested, then fresh water is pumped through the 4-1/2'' E75 16.6 lb/Ft drill pipe and the stimulation sleeves which allows to perform the stimulation job more controlled and target-oriented. The pressure required to open existing fractures will be determined with a step-rate-test by pumping through the straddle assembly in the isolated interval fresh water. After pumping fresh water and flow back, the ball drop deflation system will be activated to pull the straddle assembly out of hole. This procedure will be performed for each stage.

5) Airlift test: A second airlift test will allow to estimate the change in productivity after the stimulation treatments.

6) Open hole logging: A new set of temperature logs will be run at the end of the stimulation job in order to confirm the locations of all inflow zones. Optional, another set of logs including BHTV will be run in order to identify changes at the borehole wall (e.g., fracture slip) caused by the stimulation treatments.

3.3 Zonal isolation and target sections

Zonal isolation treatment has been selected since the whole open hole section below the 9-5/8'' Casing has already been primary stimulated. This earlier stimulation in 8-1/2'' open hole resulted in improved production rates. The new job plans to stimulate three individual smaller feed zones along the 8-1/2'' open hole. The new stimulation intervals were roughly identified based on existing information acquired from temperature logs and lithological profiles of the well. Setting depths for the inflatable packers and space out intervals for the straddle assembly and stimulation sleeves will be adjusted based on the new well logging information acquired once the rig is on site. Preliminary target intervals are shown in Table 1. Fractured and highly altered basalts will be preferred as injection intervals while unaltered and intact doleritic intrusions will serve as sealing sections for setting the packers of the straddle assembly.

3.4 Injection parameters and scheme

The differential pressure required for hydraulic fracturing (HF) is an estimation of the maximum pressure that would be required during the stimulation. This is because the pressure range for hydro-shearing is lower than the hydraulic fracturing pressure range and the stimulation job is designed for hydro-shearing. The HF pressure is calculated according to Equation 1 for a vertical impermeable borehole with the vertical stress being the maximum and assuming zero tensile strength.

$$\Delta P = 3SHmin - SHmax - Pp \quad (1)$$

The required injection rate to achieve these hydraulic fracturing pressures was estimated based on recorded wellhead pressures and flow rates during previous operations in RV-43. The initial well productivity was in the range of ~1.0-1.6 l/s/MPa was estimated from an air lift test performed after drilling operations. The injectivity increased to ~6 l/s/MPa after the earlier stimulation job performed in 2001. Therefore, an initial injectivity of ~1 l/s/MPa is assumed for each of the stages in the new stimulation job and the injectivity is expected to increase to ~3 l/s/MPa after the treatment. These injectivities and pressures lead to surface flow rates between 11.5 l/s and 48 l/s to reach the hydraulic fracturing pressure assuming no frictional pressure losses. These flow rates and differential pressures can thus be considered as maximum values or operational limites since fracturing the formation is not the main purpose of the hydro-shearing treatment.

However, the injection parameters are not only constrained by geological boundary conditions, but also by available technical equipment. In particular, the maximum stand pipe pressure of the rig is 20.7 MPa (3000 psi). To reach the required injection flow rates two pumps will be running on line in parallel. Each pump can supply a minimum flow rate of 9-15 l/s and a maximum flow rate of 18.1-29.3 l/s depending on the pump liner size. Combining two pumps with different liner sizes, the available flow rate range is thus 9-47.4 l/s. The maximum flow rate of the available water supply is estimated to be ~20 l/s. The required injection water sources are located in the two neighboring wells HS-44 and HS-33 in addition to water from the network of the city. To keep the water supply during the stimulation job continuously a water storage tank of at least 100 m³ capacity will be available at the rig site. The maximum volume that can be pumped in 24 hours is thus restricted by the water supply of ~20 l/s, which results in 1728 m³. 4 days of continuous pumping per stage thus results in a maximum injection volume per stage of ~7000 m³. Considering the technicial specifications of the equipment, available water supply and geological parameters, the estimated injection parameters for each stage are summarized in Table 1.

Table 1: Estimated injection parameters for the three different injection stages. The differential pressure required for hydraulic fracturing (HF) equals to the maximum expected pressure since lower pressures will be required for hydro-shearing. The flow rate q required for HF depends on the injectivity index (II) of the stage. It is assumed that the initial II is max. 1 l/s/MPa before the stimulation. Afterwards it is expected to increase by a factor of 2-3, resulting in an II of 3 l/s/MPa.

	Stage 1	**Stage 2**	**Stage 3**
Measured depth (m)	1700-1750	1300-1350	1100-1150
True vertical depth (m)	1467-1507	1150-1189	1001-1032
Target structure	Intersection with Gabbro	Small feed zone	Large feed zone
~SHmax (MPa)	22	18	16
~Shmin (MPa)	17.5	14.5	12.5
~Pp (MPa)	14.5	11.5	10
~ΔP required for HF (MPa)	16	14	11.5
q req. for HF with II=1 l/s/MPa (l/s)	16	14	11.5
q req. for HF with II=3 l/s/MPa (l/s)	48	42	34.5
Maximum volume (m³)	7000 m³	7000 m³	7000 m³
Maximum pumping time (days)	4	4	4

An exemplary injection scheme for one stage is shown in Figure 5. First, the fracture opening pressure (FOP) will be approached slowly and determined by increasing the flow rate stepwise with cyclic flow rate reductions. Once the FOP is known the last injection cycle will be repeated multiple times. This is followed by cyclic pulse injection where the injection volumes are the same as in the cyclic injection before. Afterwards, the same volume will be injected again with constant flow rate. A repetition of this procedure will allow comparing the seismic and hydraulic response of the reservoir to the different injection schemes, which will provide valuable input for optimization of future stimulations. In the end the flow rates and pressures will be reduced stepwise and part of the injected water will be flowed back before the next stage is going to be stimulated.

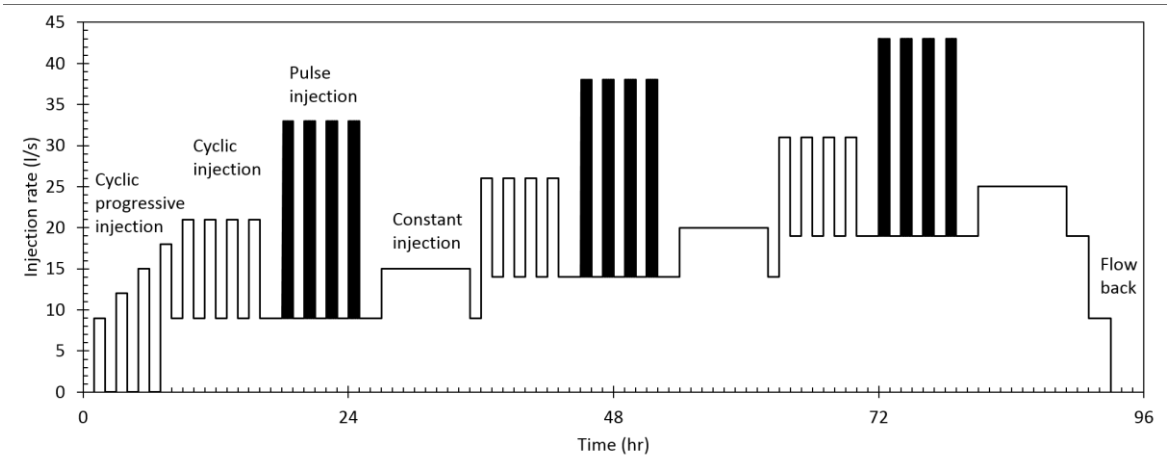

Figure 5: Exemplary injection scheme with assumed initial fracture opening at 15 l/s. The same cyclic, pulse and constant injection scheme is repeated three times with the same volume being injected during each scheme. Flow rates likely need to

be increased during the stimulation to achieve the required stimulation pressures depending on the effectiveness/efficiency of the stimulation. According to this schedule a total of ~4500 m³ of water would be injected in that stage.

4. SEISMIC MONITORING DESIGN

4.1 Seismic monitoring network

The recent seismic activity near Reykjavik is low and little is known about larger historical events. Also the knowledge about weak seismic events with M<1 is limited, due to the lack of a dedicated network. In the framework of fluid injection operations and geothermal stimulation, monitoring the migration of induced (micro-) seismicity requires precise hypocentral location and robust magnitude estimation in real-time (Grigoli et al., 2017). The detailed analysis of induced micro-seismicity in space and time as well as studies of the source parameters of small earthquakes allow to track the spatial distribution of fractures within the reservoir. It can help to identify active faults and lineaments that may trigger large induced seismic events as well as to optimize hydraulic stimulation operations and to locate the regions with higher permeability, enhancing energy production. Microseismicity analysis requires a dense local seismic network with real-time analysis capability, able to detect weak events, with magnitudes even smaller than M=0 and to support a significant statistical analysis. Micro-seismic monitoring plays a key role in better understanding the physical mechanisms governing induced seismicity (Grigoli et al., 2017). It is the fundamental tool used by decision makers to decide whether to stop, decrease, or continue the industrial operations being monitored.

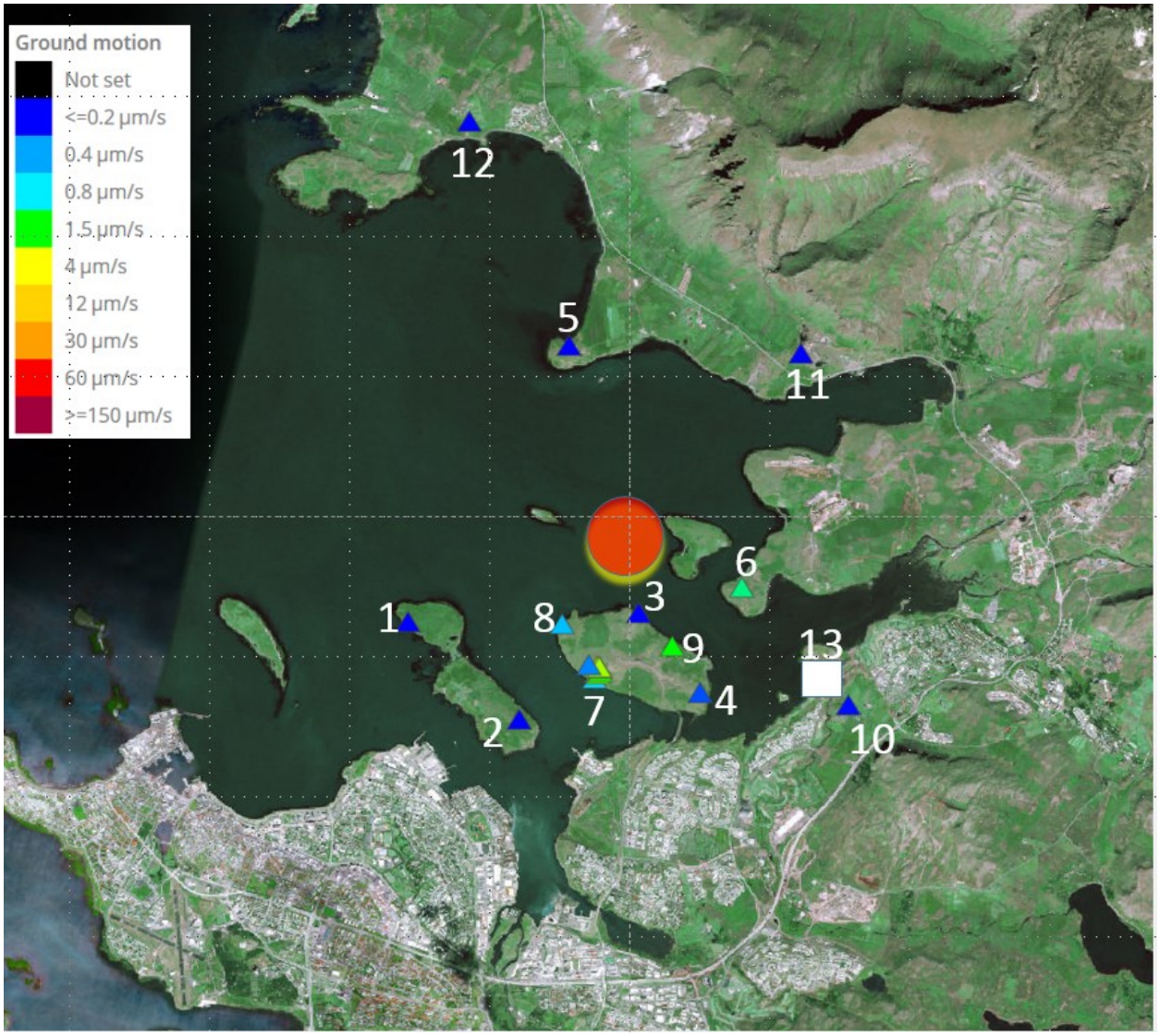

Figure 6: View of the temporary local seismic monitoring network around Geldinganes (http://veitur.isor.is/stationview/). The task of this network is the monitoring of the seismic events in the area around the future stimulation site (indicated by the larger red dot). The installation started in late 2018 with 6 short period stations (1-6 in the Table 2). Since July 2019 additional seismic stations were integrated as a small scale array (7) on the island Geldinganes and additional short period stations (8 to 12). At location 13 a borehole geophone chain was installed with 17 short period 3-component geophones with a vertical spacing of 10 meter in the depth interval 1040m to 1200 m. The distance to the stimulation area is roughly 3-4 km.

According to Catalli et al. (2013) and Zang et al. (2014) the detailed analysis of the induced seismic activity in space and time can provide a consistent picture in the near- and far-field of the stimulation well. In the beginning of the stimulation and close to the injection well, high pore pressures induce clusters of small events (seismic clouds), which are characterized by migrating fronts of seismicity and high b-values. Zang et al. (2014) suggests significant volumetric components of the source mechanisms during the

high pore pressure phase. With the expansion of the stimulated area the contribution of the fluid overpressure far from the injection point may become smaller and smaller. The volumetric component of the focal mechanism may become insignificant and the shear stress necessary to trigger an event must increase. Microseismic studies may also indicate when and where seismic events line up along (often unknown) pre-existing faults or fractures zones which may release seismic energy in larger seismic events.

In late 2018 a new local seismic monitoring network was setup around the future stimulation site with real-time communication capability. The official international network code is YG (internal name Veitur "VE"). ISOR and Reykjavik Energy (OR) set up 5 short period (1 Hz) seismic stations and instrumented 1 shallow borehole sites (stations 1-6 in Table 2). Later, the project partners improved the station coverage around the stimulation site by adding a small scale seismic array (7 stations on Geldinganes, marked as station 7 in the Table 2 and Figure 6) and additional short period seismic stations (stations 8-12). The instruments are provided by the GIPP instrument pool of GFZ Potsdam and will be removed after the stimulation period in October 2019. Data from these additional stations are also accessible online and reporting the waveform data to ISOR, like all stations, with 200 Hz (or 250Hz) sampling interval.

Besides the land surface and shallow borehole stations, a borehole geophone chain (*SlimWave*, Sercel) from GFZ Potsdam (ICDP) is installed (station 13 in Figure 6) and operational since July 22, 2019. The 17 3-component short period (15 HZ) borehole geophones were installed in the depth interval 1040 – 1200 m in well R-42. This system will also continuously monitor the ground motion until the end of the project in October 2019. The sampling rate for all components is 2 kHz. We convert the original (1 sample) overlapping SEGY files into a continuous data stream in miniSEED format, consistent with the data format of all other seismic stations. This is possible as the 15 seconds long SEGY-Files have µ-sec precise time information in their header data. All data with 2 kHz sampling from the 17 geophones are transmitted to ISOR via a network connection and are integrated as 17 seismic stations with the same location but different depth into the SC3 real-time analysis system.

Most of the surface stations are set-up on hard rock, minimizing local effects and noise amplification due to shallow soft layers. The surface stations are either placed in a barrel buried in the ground, filled partly with concrete coupled to the hard rock or are under a protective bucket covered with sand and stones which shield against direct wind contact. The stations are in a distance range from 1 to 7 km from the future stimulation area. Besides the stations listed above, data from another seismological network in the Hengill region, ~20 km to the east, is being integrated for an improved analysis.

Table 2: Seismic Stations installed as permanent and temporary stations in the frame of the DESTRESS project (Abbreviations: Short Period=SP, A=Array, 3-component=3c).

ID	Network code	Frequency	Installation	Description
1	VE.Veitur	SP, 200 Hz	Buried	Surface station, 1Hz, 3c
2	VE.Skoli	SP, 200 Hz	Buried	Surface station, 1 Hz, 3c
3	VE.Geldv	SP, 250 Hz	Borehole	122.5 [m], 1 Hz, 3c
4	VE.Gelda	SP, 200 Hz	Buried	Surface station, 1 Hz, 3c
5	VE.Brim	SP, 200 Hz	Buried	Surface station, 1 Hz, 3c
6	VE.Nidur	SP, 200 Hz	Buried	Surface station, 1 Hz, 3c
7	YG.GA1..GA7	A, SP, 200Hz	protected	Surface stations, 7 stations, 1 Hz, 3c
8	YG.Geldw	SP, 200 Hz	buried	Surface station, 1 Hz, 3c
9	YG.Gelde	SP, 200 Hz	protected	Surface station, 1 Hz, 3c
10	YG.Blika	SP, 200 Hz	protected	Surface station, 1Hz, 3c
11	YG.Esja	SP, 200 Hz	protected	Surface station, 1Hz, 3c
12	YG.Lykk	SP, 200 Hz	Borehole	25 [m], 4.5Hz, 3c
13	YG.R42	SP, 2000 Hz	Borehole	Borehole geophone chain, 1040-1200 m, 17 geophones, 15 Hz, 3c

4.2 Automatic real-time analysis

All waveform data are being transmitted with LTE communication to the *Iceland GeoSurvey* (ISOR, http://en.isor.is/) allowing for near real-time analysis for event detection, event location, magnitude evaluation as well as automatic event notification and alerting via SMS and email within seconds after an event has occurred. The automatic event detection, event location and magnitude determination is being done by a SeisComp3 system (SC3, https://www.seiscomp3.org/). This first event solution is expected to provide an absolute location accuracy of less than 100 meters, as confirmed by first tests of the network performance.

We will test different seismic velocity models to minimize the location and source mechanism errors for the Geldinganes area. The starting seismic velocity model will be based on seismic refraction profiles in the vicinity of Geldinganes (Flóvenz, 1979) and a refraction profile north of the area (Bjarnason et al., 1993). One refraction profile is just south of Geldinganes, but Geldinganes and the area north of it are in the roots of a volcanic complex with gabbroic intrusions so the velocity is expected to be higher there. These higher velocities may be presented by Tryggvason et al. (2002).

Maps and graphs of the induced seismic activity will be produced and updated by ISOR, which are needed as background information for the stimulation team and the TLS. The time from July 2019 until the stimulation phase will be used to improve the velocity model as well as the parameters for the local magnitude ML calculation. In addition, it is being planned to use an explosion NW of the stimulation site to check the velocity model, the sensor orientation of the horizontal components and the seismic station settings (amplification, meta-data).

All data are being archived at ISOR and GFZ Potsdam through the GEOFON project. Project partners of the DESTRESS project can access the real-time and the archived data as "YG" network already now, while interested scientists can access all data as archive from the "YG" network through the GEOFON Data Archive (http://eida.gfz-potsdam.de/webdc3/) at the end of the DESTRESS project.

4.3 Semi-automatic analysis in near real-time

In order to improve the automatic location accuracy as well as the extraction of important details about the source mechanism, a series of secondary processing stages is being triggered by SC3 when an earthquake was detected. These include relative earthquake location and detailed source mechanism studies. We expect an improved location accuracy of about 10m, allowing detailed monitoring of the seismicity migration. The implemented extra modules for SC3 like *scanloc* (Grigoli et al, 2018) will improve local earthquake and micro-seismicity monitoring accuracy. The *scautopick* extension S-AIC which provides automatic accurate S-picks even improves the scanloc results.

Event triggered analysis is done by additional public available software based on *Pyrocko* (Heimann et al., 2017) and *Grond* (Heimann et al., 2018, Heimann et al, 2019). *Grond* is an open source software tool for robust characterization of earthquake sources. Moment tensors and source parameters can be estimated from the inversion of seismic waveforms and waveform attributes. It delivers meaningful model uncertainties through a Bayesian bootstrap-based probabilistic joint inversion scheme. The optimization explores the full model space and maps model parameter trade-offs with a flexible design of objective functions.

As an application from the Reykjavik area, the detailed full waveform analysis of a recently reported event on 2019-06-16 at 09:42.20 with ML 1.1, located in about 21 km east to the stimulation well. For this centroid moment tensor analysis we chose the velocity model from Tryggvason et al. (2002). The semi-automatic analysis does not only give an estimation of an improved location, of the depth, the moment magnitude Mw and seismic moment, but also of the source mechanism (double couple). In this case, an oblique strike slip with reverse component is indicated.

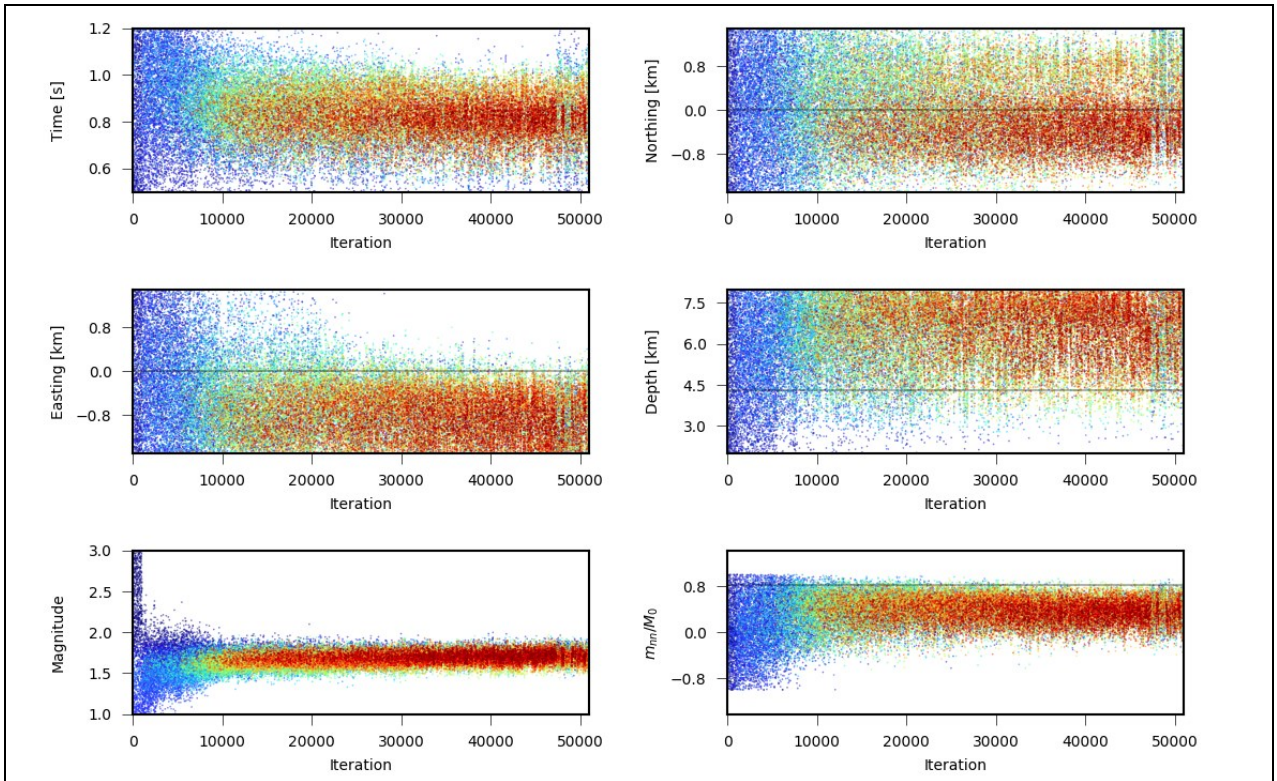

	Latitude [°N]	Longitude [°E]	Depth [km]	Magnitude	Strike	Dip	Rake	
SC3	64.022	-21.565	4.3	ML=1.1	-	-	-	
Grond	-240 m	-770 m	5.8	Mw=1.7	10 104	43 88	180 50	

Figure 7: At the end of an automated iteration of 50000 runs, the sequence of the seismological parameter values is a function of the optimization. Displayed are the results for the event time, location and depth, moment magnitude Mw and seismic moment. The improved analysis gives a slight shift in the location south and east, a depth of nearly 6 km and a double couple source mechanism.

5. SEISMIC RISK ASSESSMENT

The pre-stimulation induced-seismic hazard and risk analyses are provided in Broccardo et al. (2020). These analyses are based on a fully probabilistic framework, including epistemic and aleatory variability, different earthquake rate models (both statistical; Mignan et al. 2017 - and physics-based; Karvounis et al. 2014, Karvounis and Jenny 2016), a set of the ground motion characteristic models, a selection of vulnerability functions and the related consequence models (e.g. Mignan et al., 2015). Two risk metrics together with two risk thresholds are selected for pre-drilling decision making. The first risk metric is the individual risk (IR) with threshold of 10^{-6}, and the second is a low damage metric with a threshold equal to 10^{-2}. The individual risk is defined as the annual frequency at which a statistically average individual is expected to experience death or a given level of injury from the realization of a given hazard (Broccardo et al. 2017a; Mignan et al. 2019a; b). The low damage risk is defined as the frequency over the time span of the project at which a statistically average building class is expected to experience light non-structural damage from the realization of a given hazard, is introduced as second risk metric.

The results of the risk assessment indicate that the overall risk for an individual to die in a building within a radius of 2 km around the well is assessed to be below 10^{-7}. This value is well within the acceptable range when compared to acceptance criteria applied in the Netherlands (or Switzerland). Reason for the acceptable risk is the estimated low vulnerability of the building stock, the overall limited injection volume and the constraints posed by the 2001 injection data. The chance of damage to buildings is around 0.1% and therewith well below the 10^{-2} acceptance threshold. Moreover, the thresholds proposed in the classical traffic light (Figure 8) are consistent with the risk thresholds computed; it is not needed to define more conservative thresholds at this point. Finally, the uncertainties at this stage of the project are very high (mostly due to uncertainty on underground seismic feedback; e.g. Mignan et al. 2019b), highlighting the importance of updating the risk study continuously as new data becomes available (Broccardo et al. 2017b).

6. SEISMIC RISK MITIGATION MEASURES

6.1 Cyclic injection

It has been shown in several experiments at multiple scales that cyclic injection leads to lower magnitudes of seismic events, lower breakdown pressures and more complex fracture systems (Hofmann et al. 2018b). Depending on the frequency, this is attributed to a hydraulic fatigue effect resulting from pulse pressurization (Zang et al. 2013) and stress relaxation in between high rate injection phases (Hofmann et al. 2018a; Kwiatek et al. 2019; Zang et al. 2019). The overall goal of cyclic injection is a more controlled fracture development to increase permeability with reduced seismic risk.

6.2 Multi-stage injection

The application of multi-stage injection serves several purposes. First, the stimulation of specific intervals along the open hole section is only possible by sealing off the areas above and below the stimulation targets. In this particular well this is mandatory as the entire open hole section has already been stimulated in 2001. Second, the stimulation of multiple sections potentially leads to a higher overall productivity increase as compared to the stimulation of only one section since multiple new inflow zones are developed. Third, the seismic risk is reduced compared to a massive open hole or single-stage stimulation. This is because only smaller individual volumes are stimulated in each stage as compared to one large volume (Meier et al. 2015). One target of the RV-43 stimulation is the demonstration of this promising concept in the field.

6.3 Slow flow rate changes, limited injection rates and flow back instead of shut-in

At the start of the treatment flow rates are increased stepwise. This allows to determine the fracture opening pressure and to slowly approach critical pressures required for stimulation and inducing seismicity. Once the fracture opening pressure is known the flow rates are not increased significantly more. At the end of the treatment the flow rates are reduced slowly to avoid abrupt changes of pressures and stresses in the reservoir and part of the injected fluid is flowed back. The flow back is required as it was observed that the magnitude of induced seismic events may increase during shut-in periods after the stimulation (e.g. Basel EGS; Mukuhira et al., 2017). On the other hand, it was demonstrated that flow back instead of shut-in can lead to an immediate decrease in seismic magnitudes during the flow back period (e.g. Pohang EGS; Hofmann et al. 2019). More details on these procedures can be found in Hofmann et al. (2018).

6.4 Monitoring of volumes and energies

At several EGS projects a site-specific seismic magnitude – injection volume relationship has been observed. For example, this has been reported for one of the stimulations of the Pohang EGS, where this relationship, and the deviation from it at a certain volume, was used to constrain the maximum fluid injection volume before the stimulation to stay below a predetermined target magnitude during injection (Hofmann et al. 2018a, 2019). Afterwards it was also successfully used for real-time analysis at the Helsinki EGS project to estimate the maximum injectable volume required to stay below a similar target magnitude during injection (Kwiatek et al. 2019). During the stimulation of well RV-43, injected net volumes, injected hydraulic energies, radiated seismic energies and seismic moment magnitudes will be observed and related to each other in a similar fashion in order to be able to observe critical trends which may lead to a stop in injection before indicated by the traffic light system.

6.5 Classical traffic light system

Seismic traffic light systems (TLS) are standard procedures to manage seismic risks for fluid injection activities. In Iceland it is applied for example for re-injection activities in the Hellisheidi geothermal field (Thorsteinsson and Gunnarsson, 2014). For Geldinganes the TLS is shown in Figure 8. It is based on the TLS applied at Hellisheidi with some modifications. In addition to the conventional TLS, an advanced TLS will be applied for the first time in the field. Therefore, it cannot be used without a conventional TLS, but the more conservative of the two serves as the decision criterion.

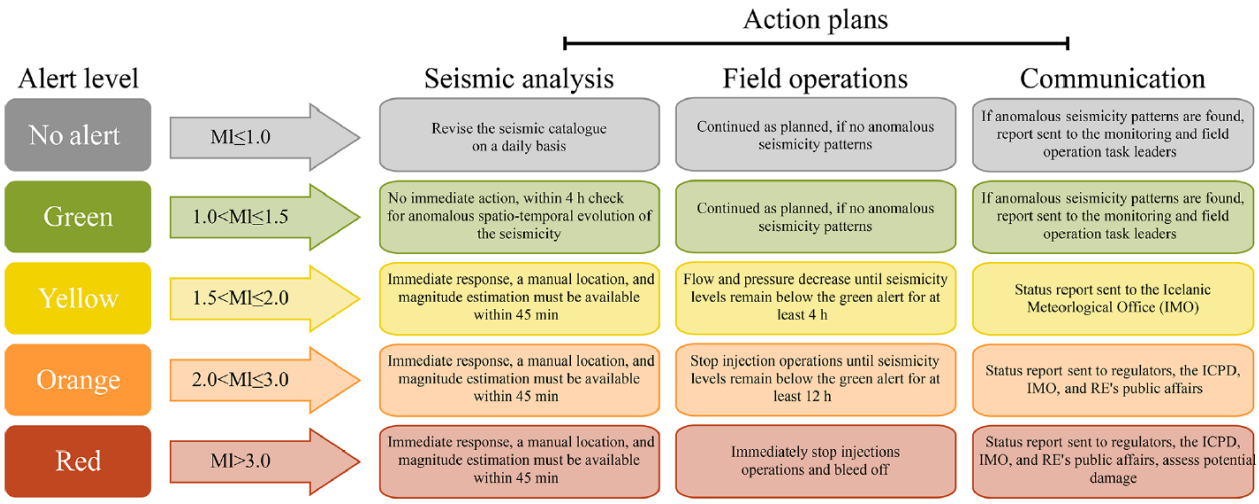

Figure 8: Traffic light system for the hydraulic stimulation of well RV-43 (Broccardo et al. 2020).

6.6 Advanced traffic light system

The proposed advanced traffic light system is based on the work of Mignan et al. (2017). In the classical TLS the definition of the magnitude threshold is based on expert judgment and regulations. Here, we propose a data-driven Adaptive TLS, ATLS, which intends to overcome the limitations of the traditional heuristic methods. In the proposed ATLS the assignment of a magnitude threshold is dynamic and based on a quantitative risk assessment, subject to a safety criterion imposed by the authorities (in this project $IR<10^{-6}$). As a consequence, the ATLS is an objective and more robust mitigation strategy, which facilitates a fair and transparent regulatory process. This approach is in line with the protocols common for most other technological risks, such as in the hydropower, nuclear or chemical industries.

The proposed statistical model includes a linear relationship between seismicity rate and flow rate (which has been used in different applications and by different research groups, see Mignan et al. 2019a; b), as well as a normal diffusion process for post-injection. The model is fully integrable yielding a closed-form ATLS solution and depends only on three physically meaningful parameters. The closed form relationship shows a direct relationship between the dynamic magnitude threshold and dynamic changes of the b-value during the injection. It follows that in the case of b-value drop, the magnitude threshold will quickly drop too to very low magnitude thresholds and stop the injection. This proves the critical role of the b-value and the importance of a dense seismic network with a low completeness magnitude, so that the value of b can be determined as early as possible during the stimulation. For the current seismic network configuration, we estimated - with the Bayesian Magnitude of Completeness (BMC) method (Mignan et al. 2011) calibrated to Icelandic conditions (Panzera et al. 2017), a completeness magnitude of c. 0.0 in the site area, which should be further improved in the near future.

7. CONCLUSIONS

A cyclic hydraulic stimulation concept for a target oriented and safe multi-stage productivity increase of well RV-43 in Reykjavik was developed. This stimulation concept is based on a site assessment with focus on previous stimulations in the area, stress field and structural geology. Critical for the success of the project is the isolation of new stimulation targets from previously stimulated high permeability zones. Due to the vicinity of the well to the city of Reykjavik, special emphasis concentrates on seismic risk assessment and mitigation. Risk mitigation measures are the application of the cyclic soft stimulation concept, multi-stage stimulation, monitoring of the injection volumes and energies, real-time seismic monitoring, a conventional seismic traffic light system and an advanced seismic traffic light system.

ACKNOWLEDGEMENTS

The authors are grateful for the funding received from the European Commission Horizon 2020 research and innovation programme under grant agreement No. 691728 (DESTRESS).

REFERENCES

Axelsson, G., Thórhallsson, S. and Björnsson, G.: Stimulation of geothermal wells in basaltic rock in Iceland, *ENGINE – Enhanced Geothermal Innovative Network for Europe Workshop 3 "Stimulation of reservoir and microseismicity"*, Zürich, Switzerland, (2006).

Bessason, B., Ólafsson, E., Gunnarsson, G., Flovenz, O., Jakobsdóttir, S., Björnsson, S. and Árnadóttir, T.: Verklag vegna örvaðrar skjálftavirkni í jarðhitakerfum, *Technical Report (In Icelandic),* Orkuveita Reykjavíkur, Reykjavik, Iceland (2012).

Bjarnason, I.T., Menke, W., Flóvenz, O.G. and Caress, D.: Tomographic Image of the Mid-Atlantic Plate Boundary in Southwestern Iceland. *Journal of Geophysical Research*, **98**, (1993), 6607-6622.

Broccardo, M., Mignan, A., Grigoli, F. et al.: Induced seismicity risk analysis of the hydraulic stimulation of a geothermal well on Geldinganes, Iceland, *Natural Hazards and Earth System Sciences*, **20**, (2020), 1573-1593.

Broccardo, M., Danciu, L., Stojadinovic, B., and Wiemer, S.: Individual and societal risk metrics as parts of a risk governance framework for induced seismicity, *16th World Conference on Earthquake Engineering*, (2017a).

Broccardo, M., Mignan, A., Wiemer, S., Stojadinovic, B. and Giardini, D.: Hierarchical Bayesian Modeling of Fluid-Induced Seismicity, *Geophysical Research Letters*, **44**, (2017b), 11357-11367.

Catalli, F., Meier, M.-A. and Wiemer, S.: The role of Coulomb stress changes for injection-induced seismicity: The Basel enhanced geothermal system, *Geophysical Research Letters*, **40**, (2013), 72–77.

Cesca, S., Grigoli, F., Heimann, S., González, Á., Buforn, E., Maghsoudi, S., Blanch, E. and Dahm, T.: The 2013 September–October seismic sequence offshore Spain: a case of seismicity triggered by gas injection?, *Geophysical Journal International*, **198**, (2014), 941–953.

DESTRESS Deliverable 5.1: Description of individual completion elements required to segment EGS reservoir section, (2017), 44 pages.

Flóvenz, Ó.G.: Jarðsveiflumælingar á höfuðborgarsvæðinu. Dýpi á lag 3. Orkustofnun/Jarðhitadeild, *Technical Report (In Icelandic),* OS79039/JHD17, Reykjavík, Iceland, (1979).

Grigoli, F., Cesca, S., Priolo, E., Rinaldi, A.P., Clinton, J.F., Stabile, T.A., Dost, B., Fernandez, M.G., Wiemer, S. and Dahm, T.: Current challenges in monitoring, discrimination, and management of induced seismicity related to underground industrial activities: A European perspective, *Reviews of Geophysics*, **55**, (2017), 310–340.

Grigoli, F., Scarabello, L., Boese, M., Weber, B., Wiemer, S. and Clinton, J.F.: Pick- and waveform-based techniques for real-time detection of induced seismicity, *Geophysical Journal International*, **213**, (2018), 868-884.

Grigoli, F., Cesca, S., Krieger, L., Kriegerowski, M., Gammaldi, S., Horalek, J. and Dahm T.: Automated microseismic event location using Master-Event Waveform Stacking, *Scientific reports*, **6**, (2016), 25744.

Gudmundsson, A., Bergerat, F., Angelier, J. And Villemin, T.: Extensional tectonics of southwest Iceland, *Bull. Soc. Géol. France*, **163**, (1992), 561-570.

Gunnarsson, K.: Magnetic measurements and upcoming drilling in Geldinganes in 2001, *Technical report (In Icelandic)*, Orkustofnun, Reykjavík, Iceland, (2001).

Gunnlaugsson, E., Frimannson, H. and Sverrisson, G.A.: District heating in Reykjavik – 70 years experience, *Proceedings,* World Geothermal Congress 2000, Kyushu - Tohoku, Japan (2000).

Haimson, B.C. and Rummel, F.: Hydrofracturing stress measurements in the Iceland Research Drilling Project drill hole at Reydarfjordur, Iceland, *Journal of Geophysical Research*, **87**, (1982), 6631-6649.

Haimson, B.C. and Voight, B.: Crustal stress in Iceland, *Pageoph*, **115**, (1977), 153-190.

Haimson, B.C. and Voight, B.: Stress measurements in Iceland, Tectonophysics, XX, (1976), 1007.

Heidbach, O., Rajabi, M., Reiter, K., Ziegler, M. and WSM Team: World Stress Map Database Release 2016. V. 1.1., *GFZ Data Services*, (2016), http://doi.org/10.5880/WSM.2016.001

Heimann, S., Vasyura-Bathke, H., Sudhaus, H., Isken, M. P., Kriegerowski, M., Steinberg, A. and Dahm, T.: A Python framework for efficient use of pre-computed Green's functions in seismological and other physical forward and inverse source problems, *Solid Earth Discuss.*, (2019), https://doi.org/10.5194/se-2019-85, in review.

Heimann, S., Isken, M., Kühn, D., Sudhaus, H., Steinberg, A., Daout, S., Cesca, S., Vasyura-Bathke, H. and Dahm, T.: Grond - A probabilistic earthquake source inversion framework. V. 1.0, *GFZ Data Services*, (2018), http://doi.org/10.5880/GFZ.2.1.2018.003

Heimann, S., Kriegerowski, M., Isken, M., Cesca, S., Daout, S., Grigoli, F., Juretzek, C., Megies, T., Nooshiri, N., Steinberg, A., Sudhaus, H., Vasyura-Bathke, H., Willey, T. and Dahm, T.: Pyrocko - An open-source seismology toolbox and library. V. 0.3, *GFZ Data Services*, (2017), http://doi.org/10.5880/GFZ.2.1.2017.001

Hemmingsen, P., Erlingsson, S. and Bessason, B.: In-situ Stresses in Icelandic rock mass – Summary of rock stress measurements, *Nordic Geotechnical Meeting*, Reykjavik, (2016).

Hofmann, H., Zimmermann, G., Farkas, M., Huenges, E., Zang, A., Leonhardt, M., Kwiatek, G., Martinez-Garzon, P., Bohnhoff, M., Min, K.-B., Fokker, P., Westaway, R., Bethmann, F., Meier, P., Yoon, K.S., Choi, J.W., Lee, T.J. and Kim, K.Y.: First field application of cyclic soft stimulation at the Pohang Enhanced Geothermal System site in Korea, *Geophysical Journal International*, **217**, (2019), 926-949.

Hofmann, H., Zimmermann, G., Zang, A. and Min, K.-B.: Cyclic soft stimulation (CSS): a new fluid injection protocol and traffic light system to mitigate seismic risks of hydraulic stimulation treatments, *Geothermal Energy*, **6**, (2018a), 33 pages.

Hofmann, H., Zimmermann, G., Zang, A., Yoon, J.S., Stephansson, O., Kim, K.Y., Zhuang, L., Diaz, M. And Min, K.-B.: Comparison of cyclic and constant fluid injection in granitic rock at different scales, *Proceedings*, 52nd US Rock Mechanics / Geomechanics Symposium, Seattle, WA, USA, (2018b), ARMA 18-691.

Huenges, H., Ellis, J., Welter, S., Westaway, R., Min, K.-B., Genter, A., Brehme, M., Hofmann, H., Meier, P., Wassing, B. and Marti, M.: Demonstration of soft stimulation treatments in geothermal reservoirs, *Proceedings*, World Geothermal Congress 2020, Reykjavik, Iceland, April 26 – May 2, (2020).

Jefferis, R.G. and Voight, B.: Fracture analysis near the mid-ocean plate boundary, Reykjavik-Hvalfjördur area, Iceland, *Tectonophysics*, **76**, (1981), 171-236.

Karvounis, D. C., Gischig, V. S. and Wiemer, S.: Towards a Real-Time Forecast of Induced Seismicity for Enhanced Geothermal Systems, *Shale Energy Engineering Conference*, (2014), 246–255.

Karvounis, D. C. and Jenny, P.: Adaptive Hierarchical Fracture Model for Enhanced Geothermal Systems, *Multiscale Modeling & Simulation*, **14**, (2016), 207–231.

Keiding, M., Lund, B., and Ánadóttir, T.: Earthquakes, stress, and strain along an obliquely divergent plate boundary: Reykjanes Peninsula, southwest Iceland, *Journal of Geophysical Research*, **114**, (2009), B09306.

Kwiatek, G., Saarno, T., Ader, T., Bluemle, F., Bohnhoff, M., Chendorian, M., Dresen, G., Heikkinen, P., Kukkonen, I., Leary, P., Leonhardt, M., Malin, P., Martínez-Garzón, P., Passmore, K., Passmore, P., Valenzuela, S. and Wollin, C.: Controlling fluid-induced seismicity during a 6.1-km-deep geothermal stimulation in Finland, *Science Advances*, **5**, (2019), eaav7224.

Meier, P.M., Rodríguez, A.A. and Bethmann, F.: Lessons Learned from Basel: New EGS Projects in Switzerland Using Multistage Stimulation and a Probabilistic Traffic Light System for the Redcution of Seismic Risk, *Proceedings*, World Geothermal Congress, Melbourne, Australia, (2015).

Mignan, A., Werner, M. J., Wiemer, S., Chen, C.-C. and Wu, Y.M.: Bayesian Estimation of the Spatially Varying Completeness Magnitude of Earthquake Catalogs, *Bulletin of the Seismological Society of America*, **101**, (2011), 1371-1385.

Mignan, A., Landtwing, D., Kaestli, P., Mena, B. and Wiemer, S.: Induced seismicity risk analysis of the 2006 Basel, Switzerland, Enhanced Geothermal System project: Influence of uncertainties on risk mitigation, *Geothermics*, **53**, (2015), 133-146.

Mignan, A., Broccardo, M., Wiemer, S. and Giardini, D.: Induced seismicity closed-form traffic light system for actuarial decision-making during deep fluid injections, *Scientific reports*, **7**, (2017), 13607.

Mignan, A., Broccardo, M., Wiemer, S. and Giardini, D.: Autonomous decision-making against induced seismicity in deep fluid injections. In: Ferrari, A., and Laloui, L. (eds), Energy Geotechnics, SEG 2018, *Springer Series in Geomechanics and Geoengineering*, (2019a), 369-376.

Mignan, A., Karvounis, D., Broccardo, M., Wiemer, S. and Giardini, D.: Including seismic risk mitigation measures into the Levelized Cost of Electricity in enhanced geothermal systems for optimal siting, *Applied energy*, **238**, (2019b), 831-850.

Mukuhira, Y., Dinske, C., Asanuma, H., Ito, T. And Häring, M.O.: Pore pressure behavior at the shut-in phase and causality of large induced seismicity at Basel, Switzerland, *Journal of Geophysical Research Solid Earth*, **122**, (2017), 411-435.

Panzera, F., Mignan, A. and Vogfjord, K. S.: Spatiotemporal evolution of the completeness magnitude of the Icelandic earthquake catalogue from 1991 to 2013, *Journal of Seismology*, **21**, (2017), 615-630.

Sæmundsson, K., Sigurgeirsson, M.Á., Hjartarson, Á., Kaldal, I., Kristinsson, S.G. and Víkingsson, S.: Geological map of Southwest Iceland, 1:100000 (2nd edition). Reykjavik: Icelandic energy research. http://jardfraedikort.is/

Steingrímsson, B., Friðleifsson, G.Ó., Gunnarsson, K., Thordarson, S., Þórhallson, S. and Hafstað, Þ.H.: Well RV-43 in Geldinganes: The terms for the well location and design, *Technical report (In Icelandic)*, Orkustofnun, Reykjavík, Iceland, (2001).

Thorsteinsson, H. and Gunnarsson, G.: Induced Seismicity – Stakeholder Engagement in Iceland, *GRC Transactions*, **38**, (2014), 879-881.

Tomasson, J. and Thorsteinsson, T.: Drillhole stimulation in Iceland, *Proceedings,* Energy Technology Conference & Exhibition 1978, Houston, TX, USA (1978).

Tryggvason, A., Rögnvaldsson, S.T. and Flovenz, Ó.G.: Three-dimensional imaging of the P- and S-wave velocity structure and earthquake locations beneath southwest Iceland, *Geophysical Journal International*, **151**, (2002), 848– 866.

Tulinius, H., Axelsson, G., Tómasson, J., Kristmanssdóttir, H. and Gudmundsson, Á.: Stimulation of well SN-12 in the Seltjarnarnes low-temperature field in SW-Iceland, *Proceedings,* 21st Workshop on Geothermal Reservoir Engineering, Stanford University, Stanford, CA, USA (1978).

Zang, A., Zimmermann, G., Hofmann, H., Stephansson, O., Min, K.-B. and Kim, K.Y.: How to Reduce Fluid-Injection-Induced Seismicity, *Rock Mechanics and Rock Engineering*, **52**, (2019), 475-493.

Zang, A., Oye, V., Jousset, P., Deichmann, N., Gritto, R., McGarr A., Majer, E. and Bruhn, D.: Analysis of induced seismicity in geothermal reservoirs – An overview, *Geothermics*, **52**, (2014), 6–21.

Zang, A., Yoon, J.S., Stephansson, O. and Heidbach, O.: Fatigue hydraulic fracturing by cyclic reservoir treatment enhances permeability and reduces induced seismicity, *Geophysical Journal International*, **195**, (2013), 1282-1287.

Ziegler, M., Rajabi, M., Heidbach, O., Hersir, G.P., Ágústsson, K., Árnadóttir, S. and Zang, A.: The stress pattern of Iceland, *Tectonophysics*, **674**, (2016), 101-113.